Scientia Iranica A (2015) 22(2), 388–399

Sharif University of Technology
Scientia Iranica
Transactions A: Civil Engineering
www.scientiairanica.com

Investigation of bond slip effect on the P-M interaction surface of RC columns under biaxial bending

S.Sh. Hashemi* **and M. Vaghefi**

Department of Civil Engineering, Persian Gulf University, Bushehr, Iran.

Received 23 February 2014; received in revised form 3 April 2014; accepted 18 August 2014

KEYWORDS
Bond-slip effect;
P-M interaction surface;
Biaxial bending;
Reinforced concrete columns;
Seismic analysis;
Column capacity.

Abstract. The nonlinear behavior of reinforced concrete columns subject to biaxial bending and consideration of bond-slip at the steel-concrete interface are investigated. Separate degrees of freedom are used for the steel and concrete parts to allow for the difference in displacement between the reinforcing bars and the surrounding concrete. The effect of bond-slip is investigated on the numerical bearing capacity of a reinforced concrete column subject to axial and biaxial bending forces. The axial force-bending moment (P-M) interaction surface of the reinforced concrete column under two conditions (with and without bar slip) is calculated, and compared also with ACI criteria. The results show that although ACI criteria is based on perfect bond assumption, the results are conservative anyway, due to the fact that the beneficial effect of stirrup confinement on concrete compressive strength is neglected, and the use of reduction factor φ does not make any modification necessary for considering the bond-slip effect on the ultimate capacity of the RC section.

1. Introduction

Columns are the most critical part of any building or any structural skeletal frame system. A Reinforced Concrete (RC) column may be subject to biaxial bending, or to an axial load acting eccentrically, with respect to both principal axes of the cross section. The design of the column then requires computation of the failure surface of the cross section, expressed in terms of the resisting axial load and of the components of the resisting bending moment about the principal axes.

To date, many numerical methods have been proposed by researchers for calculating the bearing capacity of RC sections and for determination of the interaction diagram, which is commonly known as the P-M interaction curve or surface, under any uniaxial or biaxial bending conditions. Most design charts available today are only for the uniaxial bending of columns. The development of design charts for the biaxial bending of columns will provide structural designers with an alternative way to analyze and design such column sections. This will not only make the design easier, but will also increase accuracy, which, in turn, will provide greater structural safety. In the course of developing the design charts, a better understanding of the behavior of biaxially loaded columns will be achieved. It is possible to simplify the problem of biaxial design and analysis by generating the failure surface by means of suitable numerical formulations. Most of these methods assume that the bond between the reinforcing bars and the surrounding concrete is perfect and the slip is neglected [1-9]. This assumption, however, is not very appropriate and realistic, and causes a considerable difference between numerical and experimental results [10].

Using analytical relations and simplifying assumptions, the P-M interaction surface can be calcu-

*. *Corresponding author. Tel.: +98 771 4222150; Fax: +98 771 4540376*
E-mail addresses: sh.hashemi@pgu.ac.ir (S.Sh. Hashemi); vaghefi@pgu.ac.ir (M. Vaghefi)

lated based on the biaxial behavior. In the present study, for stocky concrete columns that are not affected by second-order effects, the role played by bond-slip on the axial force-biaxial bending moment interaction surface, is investigated. The interaction surface is calculated by considering or neglecting the bond-slip effect and the results of these two assumptions are compared; comparisons are also carried out with the criteria provided by ACI [11].

Based on ACI criteria [11], the column capacity interaction surface is numerically described by a series of discrete points that are generated on the three-dimensional interaction failure surface. A typical interaction surface is shown in Figure 1. The coordinates of these points are determined by considering a suitable number of linear distributions of the normal strain on the section of the element, as shown in Figure 2. The linear strain diagram is limited by the maximum concrete strain, ε_c, at the extremity

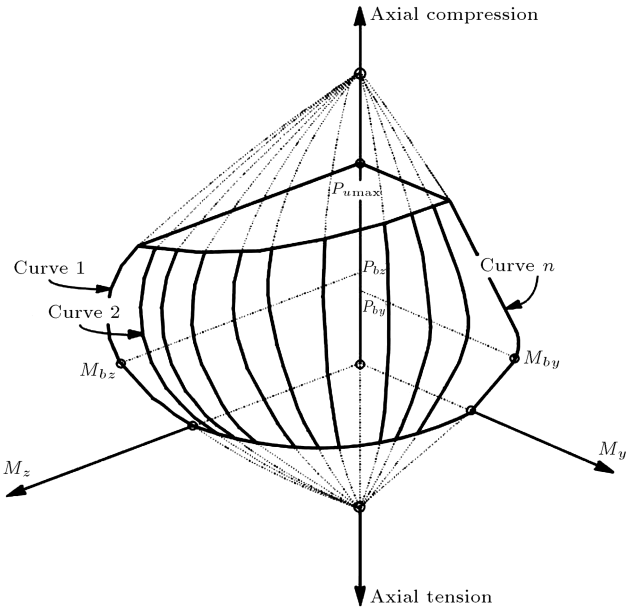

Figure 1. A typical axial force-biaxial bending moment interaction surface.

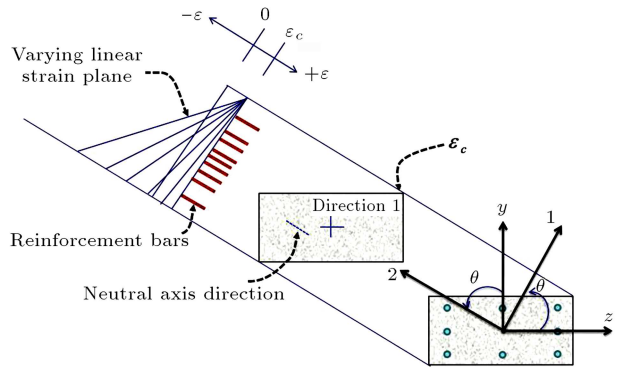

Figure 2. Idealized strain distribution for generation of interaction surface.

of the section, to 0.003. This formulation is based consistently upon the general principles of ultimate strength design. The stress in the steel is given by the product of the steel strain and the steel modulus of elasticity, $\varepsilon_s E_s$, and is limited by the yield stress of the steel, f_y. The area associated with each reinforcing bar is assumed to be placed at the actual location of the center of the bar, and the algorithm does not assume any further simplifications, with respect to distributing the area of steel over the cross-section of the column.

The concrete compression stress block is assumed to be rectangular, according to Whitney's rectangular block, with a stress value of $0.85f'_c$, as shown in Figure 3. Complementary parameters are described in ACI318-11. The interaction algorithm provides correction to account for the concrete area that is replaced by reinforcement in the compression zone. The effect of the reduction factor, φ, is included in the generation of the interaction surface for calculating the ultimate capacity of the section. The value of φ used in the interaction diagram varies between 0.65 and 0.90, under compression controlled to tension controlled conditions [11].

Following the indications of ACI318-11, P-M interaction curves are calculated on the basis of the following assumptions:

- √ The strain distribution on the reinforced concrete cross section is linear.
- √ The shear deformations are considered negligible.
- √ There is a perfect bond between the reinforcing bars and the surrounding concrete.

In this way, the P-M interaction surface, based on the perfect compatibility between concrete and bar deformations in an RC section, will be calculated (Figure 3(c)). In other words, the bond between the concrete and bars is assumed to be perfect and the slip is disregarded. In real columns, however, the bond between concrete and steel is not perfect, and the ensuring slip may affect bearing capacity estimation (Figure 3(d)).

2. Nonlinear modelling of RC columns with bond-slip effect

Many numerical models have been devised for nonlinear analysis of reinforced concrete frames. One of the most commonly used methods is the fiber model [12]. In this method, an element is divided into a number of concrete and steel fibers, and the element section specifications are worked out by adding up the effects of fiber behavior. This method assumes a perfect bond between the concrete and the bar. Limkatanyu and Spacone have used the fiber model, but they have

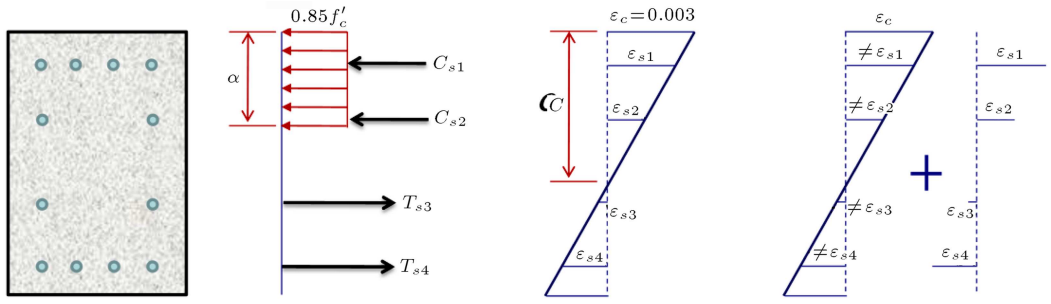

(a) Cross-section (b) Stress distribution (ACI) (c) Strain diagram (ACI) (d) Strain diagram (Considering slip effect)

Figure 3. Idealization of stress and strain distribution in a rectangular RC section.

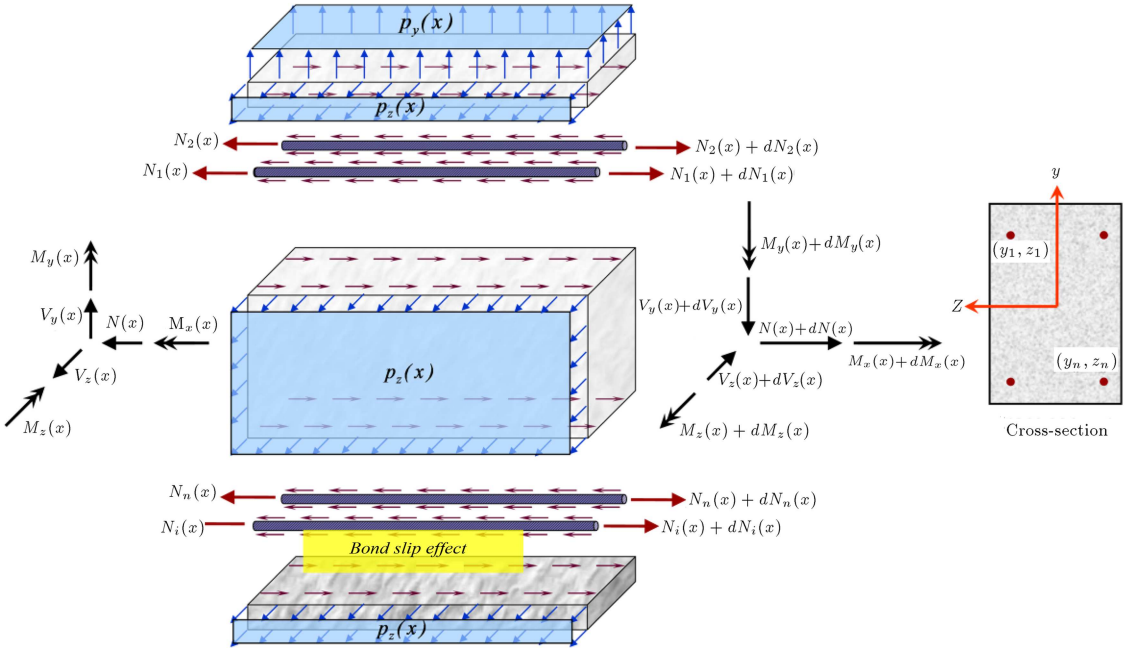

Figure 4. Free body diagram of infinitesimal segment of beam-column element and its components.

removed the perfect bond assumption [13]. In order to achieve this goal, they have separated the degrees of freedom of the concrete from those of the bars in the beam-column elements under uniaxial bending. Hashemi et al. used a similar approach and developed it for biaxial bending. They have also used a joint element, which is compatible for assembly with beam-column elements [14,15].

The free body diagram of an infinitesimal segment, dx, of the beam-column element is shown in Figure 4. Each element is introduced as a combination of one 2-node concrete frame element and n elements of 2-node bars with bond interfaces. All equilibrium conditions are written by taking into account the usual small deformation assumption. Consideration of the axial equilibrium of the concrete element and steel bars, as well as the vertical and moment equilibriums of segment, dx, leads to the matrix form of equations that are given in Eq. (1):

$$\partial_B^T \mathbf{D}_B(x) - \partial_b^T \mathbf{D}_b(x) - \mathbf{P}(x) = 0, \tag{1}$$

where:

$$\mathbf{D}_B(x) = \left\{ \overline{\mathbf{D}}(x) : \overline{\overline{\mathbf{D}}}(x) \right\}^T,$$

is the vector containing the section forces on the beam-column element.

$$\overline{\mathbf{D}}(x) = \{N(x)\ M_z(x)\ M_y(x)\ M_x(x)\}^T,$$

is the vector containing the section forces on the concrete element.

$$\overline{\overline{\mathbf{D}}}(x) = \{N_1(x)...N_n(x)\}^T,$$

is the vector of the axial forces in the bars.

$$\mathbf{D}_b(x) = \{D_{b1}(x)...D_{bn}(x)\}^T,$$

is the vector of bond section forces.

$$\mathbf{P}(\mathbf{x}) = \{0\ p_y(x)\ p_z(x)\ T(x)\ 0...0\}^T,$$

is the force vector of the beam-column element.

Moreover, n is the number of longitudinal bars in the cross section, $p_y(x)$ and $p_z(x)$ are external loads in y and z directions, respectively, $T(x)$ is the torsion load on the element, and ∂_B, ∂_b are differential operators, which are defined in the following way:

$$\partial_B = \begin{bmatrix} \frac{d}{dx} & 0 & 0 & 0 & 0 & \cdots & 0 \\ 0 & \frac{d^2}{dx^2} & 0 & 0 & 0 & \cdots & 0 \\ 0 & 0 & \frac{d^2}{dx^2} & 0 & 0 & \cdots & 0 \\ 0 & 0 & 0 & \frac{d}{dx} & 0 & \cdots & 0 \\ \cdots & \cdots & \cdots & \cdots & \cdots & \cdots & \cdots \\ 0 & 0 & 0 & 0 & 0 & 0 & \frac{d}{dx} \end{bmatrix}, \quad (2)$$

$$\partial_b = \begin{bmatrix} -1 & y_1\frac{d}{dx} & z_1\frac{d}{dx} & 0 & 1 & \cdots & 0 \\ \cdots & \cdots & \cdots & \cdots & \cdots & \cdots & \cdots \\ -1 & y_n\frac{d}{dx} & z_n\frac{d}{dx} & 0 & 0 & \cdots & 1 \end{bmatrix}, \quad (3)$$

8where, (y_n, z_n) is the coordinate of the nth bar in the section.

The slips of bars in the section of the RC element are determined by the following relation between the bar and concrete element displacements:

$$u_{bi}(x) = u_i(x) - u_1(x) + y_i\frac{du_2(x)}{dx} + z_i\frac{du_3(x)}{dx}, \quad (4)$$

where, $u_i(x)$ is bar axial displacement, and $u_1(x)$, $u_2(x)$, and $u_3(x)$ are displacements in axial, transverse in y, and z directions of the concrete element, respectively. The weak form of the displacement based finite element formulation is determined through the principle of stationary potential energy. The nodal displacement of the beam-column element, shown in Figure 5, serves as primary element unknowns, and the section displacements are related to it through the displacement shape function matrix.

A joint element is used as the footing connection of the column. In this element, the effect of pull-out can be considered as the relative displacement between the steel bar and surrounding concrete, and bond stress is referred to as the shear stress acting parallel to an embedded steel bar on the contact surface between the reinforcing bar and concrete. The number of degrees of freedom in the side of the joint element is compatible with the degrees of freedom at the ends of the column elements adjacent to the joint element. Referring to Figure 6, the slip of the bars can be defined in the form of Eq. (5), if the nodal displacement vector related to pull-out behavior is defined as:

$$\mathbf{U}_{\text{slip}} = \begin{bmatrix} U_1^2 & U_2^2 & U_3^2 & V_1^2 & ... & V_n^2 \end{bmatrix}^T,$$

$$\mathbf{slip} = \begin{bmatrix} s_1 \\ s_2 \\ . \\ s_n \end{bmatrix}$$

$$= \begin{bmatrix} -1 & 0 & 0 & 0 & z_1 & y_1 & 1 & 0 & \cdots & 0 \\ -1 & 0 & 0 & 0 & z_2 & y_2 & 0 & 1 & \cdots & 0 \\ \cdots & \cdots & \cdots & \cdots & \cdots & \cdots & \cdots & \cdots & \cdots & \cdots \\ -1 & 0 & 0 & 0 & z_n & y_n & 0 & 0 & \cdots & 1 \end{bmatrix} U_{\text{slip}}. \quad (5)$$

In this equation, (y_n, z_n) is the coordinate of the nth bar in the section. The relationship between the pull-out force and the slip for embedded bars derives from the bond stress-slip relationship related to the pull-out behavior, the embedded length of the bar, and conditions at the end of the bar and perimeter of the bar cross-section.

Further details about the modeling of joint and column modeling can be found in [14,15]. A computer program created in MATLAB software was used by the authors [16]. Selected models with good simulation accuracy for the behavior of materials and their interaction are described in Table 1.

3. Numerical investigation

For numerical investigation, numerical validation has been undertaken for a reinforced concrete stocky column, with geometric specifications according to

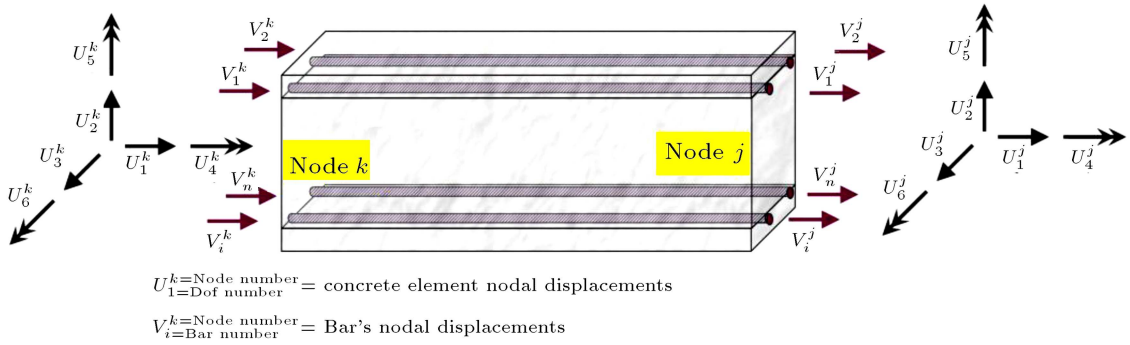

Figure 5. Three-dimensional reinforced concrete beam-column element.

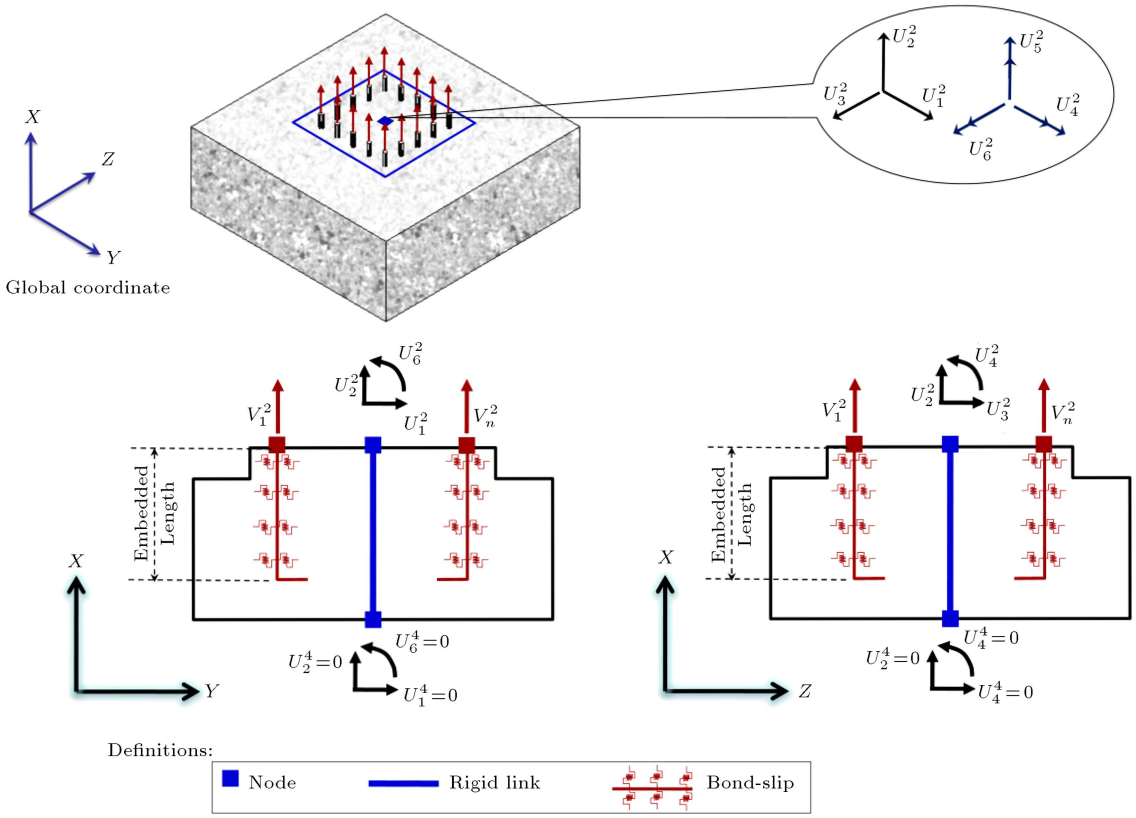

Figure 6. Three-dimensional joint element as footing connection.

Table 1. Selected models for material behavior and their interactions.

Relationship	Description
Concrete stress-strain	• The model of Park et al. [17] and later extended by Scott et al. [18] for monotonic compressive envelope curve; • It is assumed that concrete behavior is linearly elastic in the tension region before the tensile strength and beyond that; the tensile stress decreases linearly with increasing tensile strain; • Yassin [19] rules are adopted for hysteresis behavior.
Steel stress-strain	• The initially proposed model by Giuffre and Pinto [20] and later used by Menegoto and Pinto [21].
Bond stress-bond slip	• Eligehausen et al. model [22]

Figure 7, and details provided under the name of specimen 2 in Table 2. This specimen is a column under biaxial bending and constant axial load with magnitude of 350 kN. Lateral cyclic displacement was imposed at the free end with θ equal to 38.66 degrees, as tested by Qiu et al. [23]. In the numerical modeling, the column is subdivided into a suitable number of shorter elements. As the formulation is displacement based and the response depends on the element size, a large number of elements is required to ensure proper accuracy. As a simple suggestion, the length of the column elements can be selected smaller than, or equal to, the average crack spacing in the column [24]. In these cases, convergence of the calculated responses will be achieved in the numerical process. The minimum required embedded length is satisfied in all specimens in order to prevent the pull-out of the bars from the footing connection, which affects the results. Considering the ACI criteria for embedded length prevents the pull-out of the bars from the footing connection [25].

For nonlinear solving of this model, the Newton-Raphson Method, which involves controlling displacement, was used. Figure 8 shows the numerical and ex-

perimental load-displacement history with good agreement for strength and stiffness during cyclic loading.

After ensuring the accuracy and precision of the numerical method, the interaction surface of the column section for the two cases of with and without bar slip, respectively, have been calculated and compared, also with the ACI318-11 criteria. The results for specimens 1 to 3 are presented in Figures 9 to 11

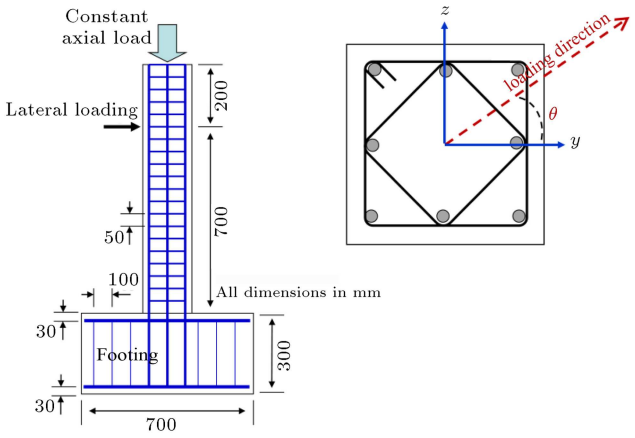

Figure 7. Geometry of the specimens [23].

through discrete curves instead of a three-dimensional surface. In these figures, M_y and M_z are the bending capacities about the y and z axes of the section, respectively, and M_t is the vector sum of M_z and M_y. Based on ACI 318-11 criteria, two additional curves are drawn in the figures: one without a reduction factor, which is known as factor φ and represents nominal capacity, and the other drawn with the effect of reduction factor φ, which represents the ultimate design capacity of the section. The latter is used to evaluate the capacity of the section in the design of reinforced concrete structures. The curve is plotted for different angles of θ because of its dimensional nature.

A summary of the evaluation and comparison of the results is listed in Table 3, where the numerical results are compared with each other, as well as with the ACI criteria. With reference to the numerical capacity, which is calculated taking into account the bond slip effect, interpretation of the results allows one to draw the following conclusions:

√ Pure axial compressive force condition: The numerical capacity for two cases of with and without slip effect will be the same. Based on ACI criteria,

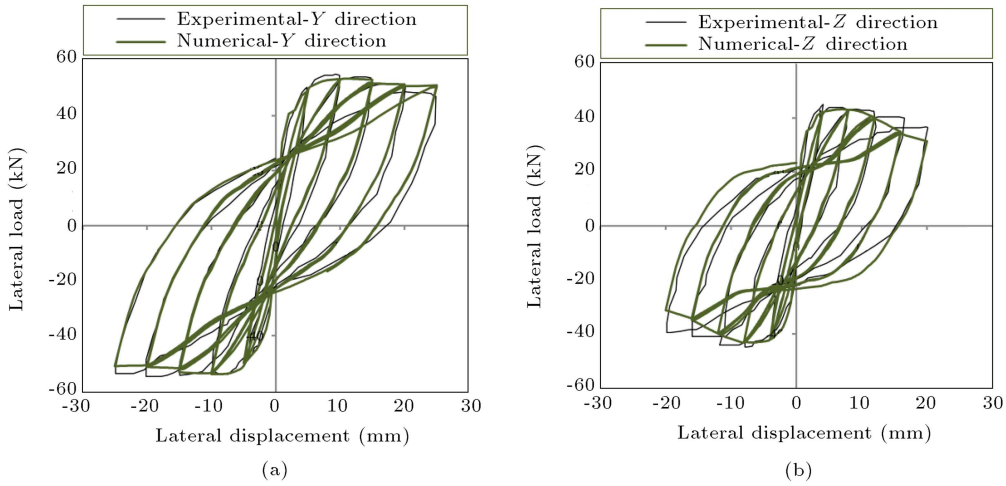

Figure 8. Experimental and numerical cyclic load-displacement responses for specimen 2.

Table 2. Details of investigated specimens.

	Specimen 1	**Specimen 2**	**Specimen 3**
	$\rho = 1.57\%$	$\rho = 2.26\%$	$\rho = 3.39\%$
Main bars	8 × 10 mm Bars	8 × 12 mm Bars	12 × 12 mm bars
Stirrups	6 mm bars @ 50 mm c/c	6 mm bars @ 50 mm c/c	6 mm bars @ 50 mm c/c
Cross-section (width*depth)	200 × 200 mm^2	200 × 200 mm^2	200 × 200 mm^2
f_c (MPa)	40	40	40
f_y of main bars (MPa)	460	460	460
f_y of stirrups (MPa)	420	420	420
Concrete cover (mm)	21	21	21

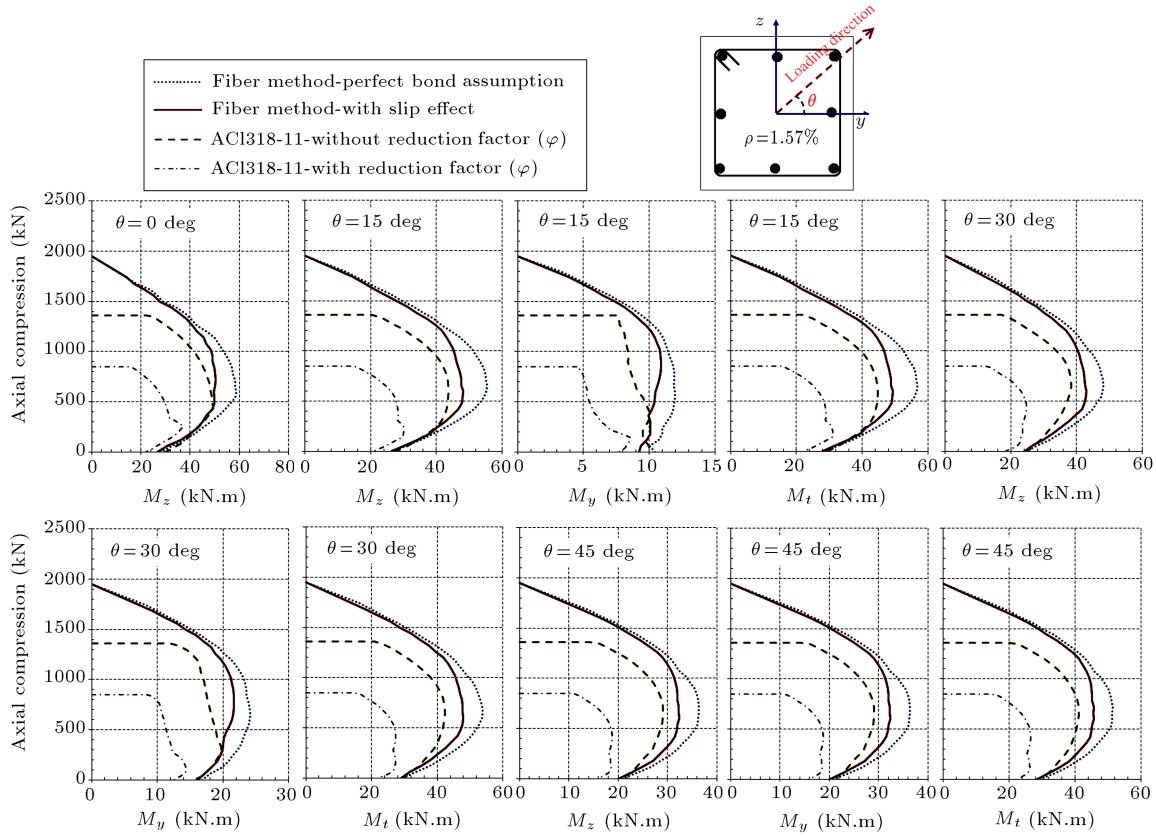

Figure 9. P-M interaction curves calculated for specimen 1.

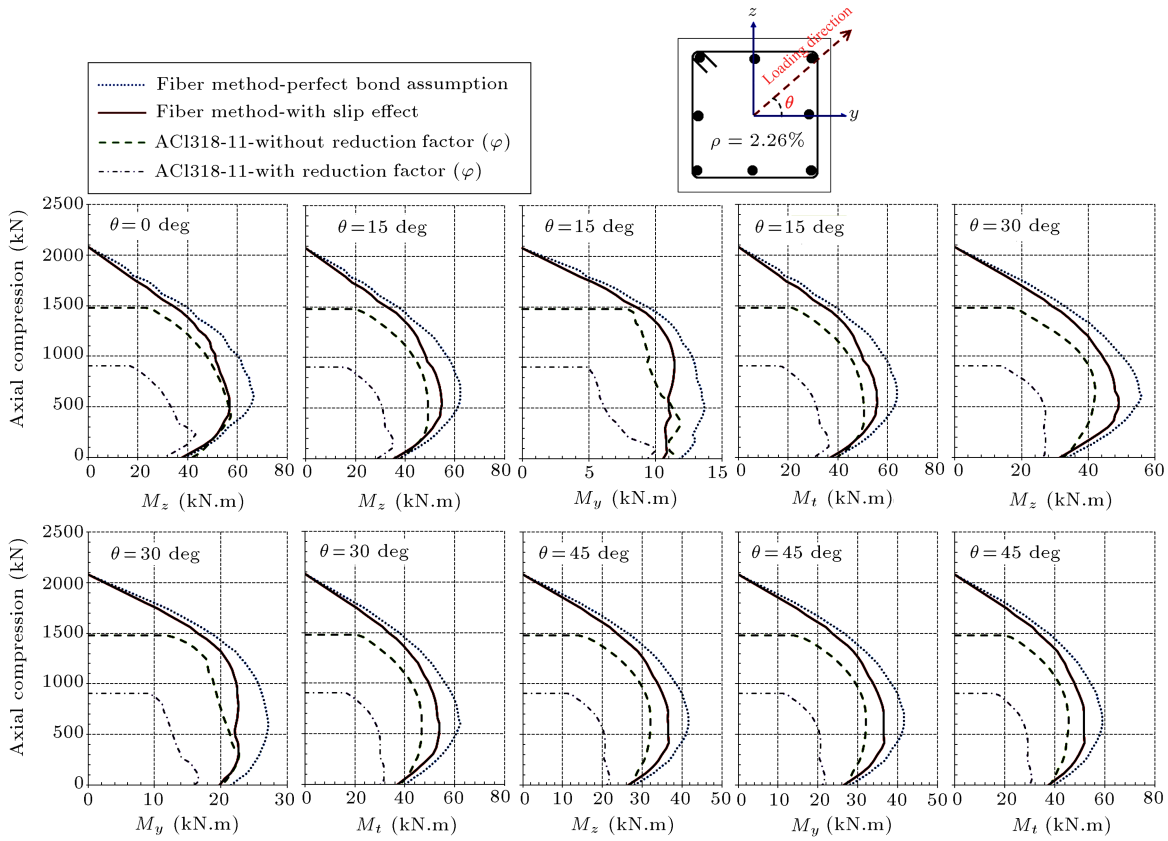

Figure 10. P-M interaction curves calculated for specimen 2.

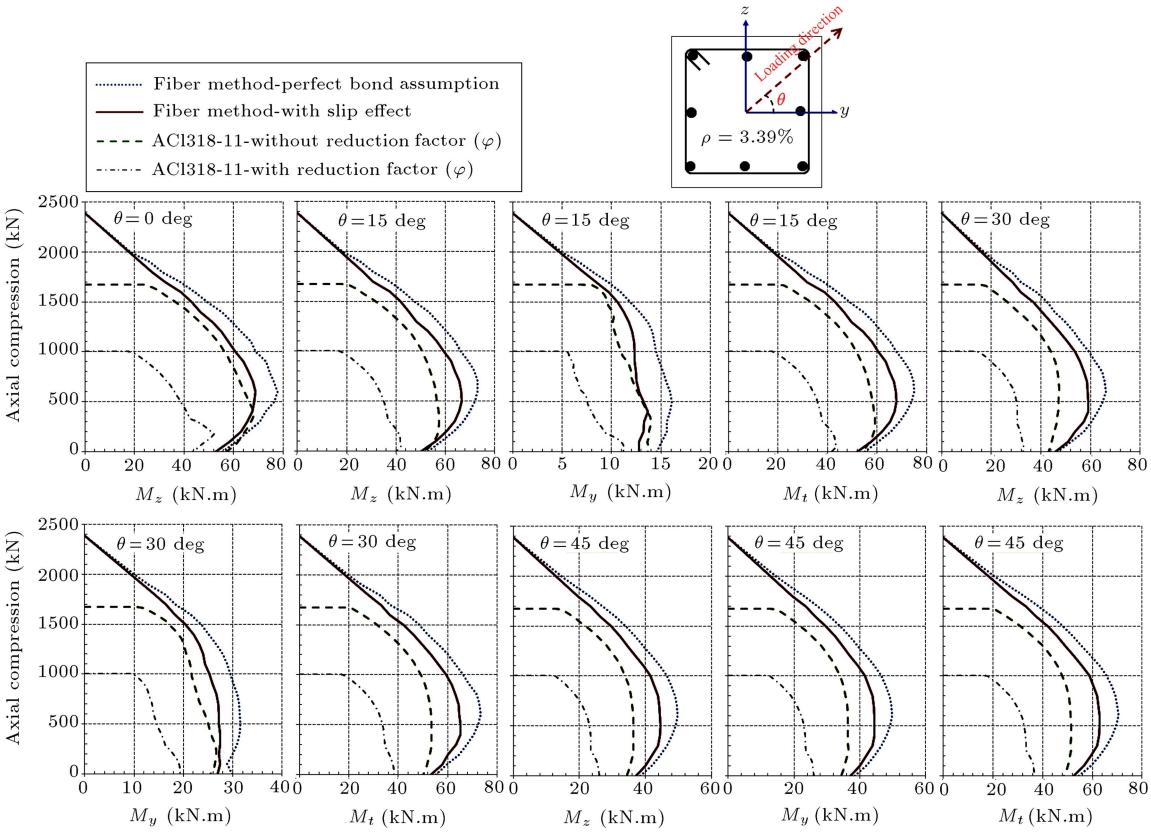

Figure 11. P-M interaction curves calculated for specimen 3.

the nominal capacity (calculated capacity without reduction factor φ) is conservative, and ensures approximately 30% less than numerical capacity. The ultimate capacity of the section (calculated capacity after applying reduction factor φ), which represents the ultimate design capacity, is more conservative and ensures approximately 56% less than numerical capacity.

√ Pure bending condition: This case will be usually used for beams under uniaxial or biaxial bending. In this condition, the numerical capacity with perfect bond assumption is only about 6% more than that obtained considering the slip effect. On the other hand, since ACI does not consider the bond-slip effect in the capacity estimation explicitly, the ACI nominal capacity is approximately 11% more than the numerical capacity and surely not conservative. However, consideration of the reduction factor leads to calculation of the ultimate capacity of the section approximately 18% lower than numerical capacity. This margin will be conservative enough without the need to include any modification.

√ Axial force with biaxial eccentricity: In this case, by investigating the state corresponding to the maximum bending capacity, the perfect bond assumption leads to a considerable difference in the capacity estimation, since the capacity will be approximately 17% larger than when the slip effect is considered. For uniaxial bending conditions, ACI nominal capacity is approximately equal to the numerical value without considerable difference. Furthermore, this difference for the ultimate capacity is about 24% and this margin will be conservative enough. For biaxial bending conditions, although ACI does not consider the bond-slip effect in the capacity estimation explicitly, the ACI nominal capacity is approximately 10% lower than the numerical capacity and surely conservative. However, consideration of the reduction factor leads to calculation of the ultimate capacity of the section approximately 42% lower than numerical capacity. This margin will be conservative enough without the need to include any modification.

By reviewing ACI 318-11 formulations, the major cause of noncompliance is that the increasing effect of stirrups on concrete compressive strength has not been considered in the ACI formulations. But, in numerical analysis, the confinement effect has been considered on the behavior of concrete fibers. For ductile RC sections and in pure bending mode, or in the presence of a very low axial force, as a rule, to reach nominal bending capacity, the bars yield with concrete compressive strength playing no significant

Table 3. Summary of numerical results for the specimens.

			Pure bending capacity		**Point with maximum bending capacity**				**Pure compressive axial capacity**
			$\theta = 0^\circ$	$\theta = 45^\circ$	$\theta = 0^\circ$		$\theta = 45^\circ$		
			M_t (kN.m)	M_t (kN.m)	M_t (kN.m)	P (kN)	M_t (kN.m)	P (kN)	P (kN)
$\rho = 1.57\%$ (Specimen 1)	Fiber method with slip effect	Value	26.6	28.4	50.5	720.0	45.7	600.0	1950.0
	Fiber method with perfect bond assumption	Value	27.8	29.4	58.7	600.0	51.4	700.0	1950.0
		Relative diff.*	4.5%	3.5%	16.3%	-16.7%	12.5%	16.7%	0.0%
	ACI318-11-without reduction factor (φ)	Value	29.9	28.6	49.4	442.9	41.2	639.0	1359.8
		Relative diff.	12.4%	0.7%	-2.1%	-38.5%	-9.8%	6.5%	-30.3%
	ACI318-11-with reduction factor (φ)	Value	21.9	22.7	37.2	255.0	26.6	413.0	846.3
		Relative diff.	-17.7%	-20.1%	-26.3%	-64.6%	-41.8%	-31.2%	-56.6%
$\rho = 2.26\%$ (Specimen 2)	Fiber method with slip effect	Value	37.8	37.5	56.8	540.0	51.7	720.0	2080.0
	Fiber method with perfect bond assumption	Value	38.8	39.8	66.6	600.0	58.9	600.0	2080.0
		Relative diff.	2.6%	6.2%	17.3%	11.1%	14.0%	-16.7%	0.0%
	ACI318-11-without reduction factor (φ)	Value	42.0	37.8	57.5	426.7	45.4	664.7	1479.0
		Relative diff.	11.1%	0.9%	1.2%	-21.0%	-12.1%	-7.7%	-28.9%
	ACI318-11-with reduction factor (φ)	Value	30.8	29.7	43.4	229.7	29.3	372.1	907.0
		Relative diff.	-18.6%	-20.7%	-23.7%	-57.5%	-43.4%	-48.3%	-56.4%
$\rho = 3.39\%$ (Specimen 3)	Fiber method with slip effect	Value	52.8	52.6	69.0	600.0	62.9	500.0	2390.0
	Fiber method with perfect bond assumption	Value	55.8	54.5	77.8	600.0	70.4	600.0	2390.0
		Relative diff.	5.5%	3.7%	12.8%	0.0%	11.8%	20.0%	0.0%
	ACI318-11-without reduction factor (φ)	Value	57.2	48.6	68.3	402.0	51.4	499.9	1674.9
		Relative diff.	8.3%	-7.6%	-1.0%	-33.0%	-18.3%	0.0%	-29.9%
	ACI318-11-with reduction factor (φ)	Value	43.5	36.8	52.2	175.8	36.8	0.0	1007.6
		Relative diff.	-17.7%	-30.1%	-24.3%	-70.7%	-41.6%	-100.0%	-57.8%

* Relative difference between values calculated with and without slip effect. Positive sign means value with perfect bond assumption is more.

role. So, the role of concrete compressive strength in the nominal capacity of the section is small and the yielding of the bars is more effective. Another cause for noncompliance between numerical capacity and the ACI curve is that the method employed in numerical analysis is based on fiber theory, including the bond-slip effect, while ACI uses the assumption of a compression block in the section. Naturally, these two methods are not identical.

In Figure 12, the numerical curves are compared with ACI. But the increasing effect of confinement on concrete compressive strength at the core of the section is considered in calculation of the ACI curve. The results show that although ACI does not consider the

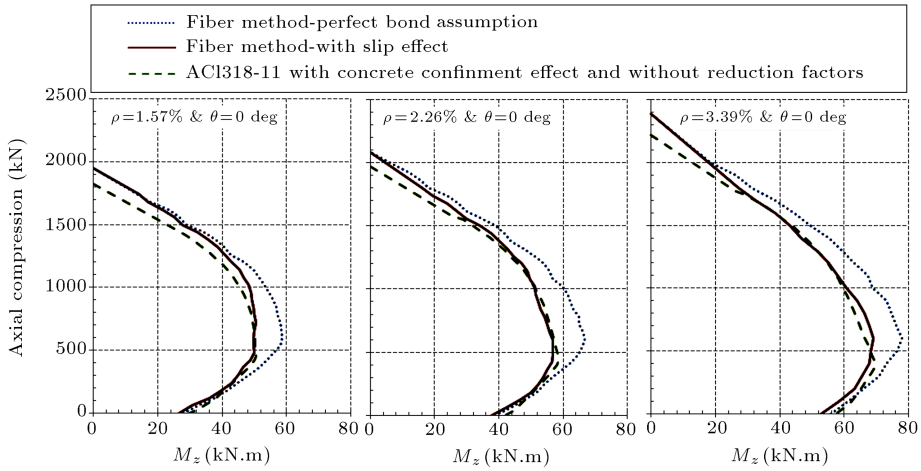

Figure 12. Comparison of numerical results with ACI curve including confinement effect of stirrups.

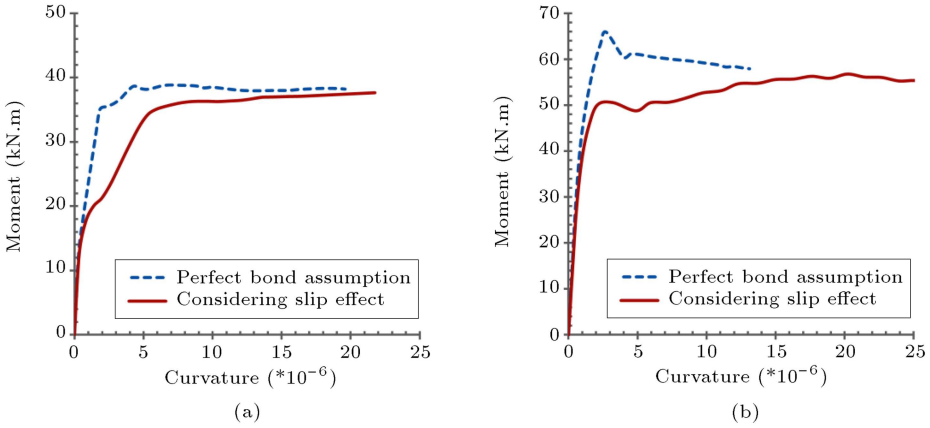

Figure 13. Uniaxial Moment-curvature curve calculated in the cross-section with zero distance to footing for specimen 2: (a) Pure bending; and (b) in the presence of axial compressive force equal to 560 kN.

slip effect, it has good conformity with the numerical curve.

Based on the results, although the ACI 318-11 criteria is based on the perfect bond assumption, the results are conservative anyway, due to the fact that the beneficial effect of stirrup confinement on the concrete compressive strength is neglected, and the use of reduction factor φ does not make any modification necessary for considering the bond-slip effect on the ultimate capacity of the RC section.

When the capacity for the two cases of with and without bar slip effect is approximately the same (for example, under pure bending conditions), it does not mean that the perfect bond assumption will not affect the accuracy of numerical responses. The moment-curvature curve of the critical cross section of specimen 2 is presented in Figure 13. In pure bending mode, as in Figure 13(a), although, in both cases of analysis, the moment capacities are approximately the same, these values correspond to different curvatures. This difference is a result of the slip effect between the reinforcing bar and the surrounding concrete. So, under such conditions, removing the slip effect further affects ductility but has no significant effect on bearing capacity. But, in the presence of an axial force with bi-axial or uniaxial eccentricity, as shown in Figure 13(b), the difference and noncompliance will be apparent for both cases of curvature and capacity, just as perfect bond assumption leads to lower ductility and higher bearing capacity estimation.

4. Conclusions

- The numerical bearing capacity under pure axial compressive force conditions will be the same for the two cases of with and without slip effect.
- Removing the slip effect under pure bending conditions has a significant effect on ductility, as well as a negligible effect on strength bearing capacity.
- In the presence of an axial force with biaxial or uniaxial eccentricity, the difference and noncompliance will be apparent for both cases of curvature and capacity, just as the perfect bond assumption leads

to considerably lower ductility and higher capacity estimation. In these cases, the capacity will be approximately 17% larger than when the slip effect is considered.

- Although the ACI318-11 criteria is based on the perfect bond assumption, and in some cases, such as pure bending mode, the nominal bearing capacity proposed by the ACI is slightly larger than the numerical one, including slip effect, the results are conservative anyway, due to the fact that the beneficial effect of stirrup confinement on concrete compressive strength is neglected. Moreover, the use of reduction factor φ does not make any modification necessary for considering the bond-slip effect on the ultimate capacity of RC sections.

Acknowledgment

This research was supported by Grant PGU/FE/17-2-1391/321 of the offices of the Vice President of Research at the Persian Gulf University. The authors are also grateful for their financial aid.

References

1. Alfano, G., Marmo, F. and Rosati, L. "An unconditionally convergent algorithm for the evaluation of the ultimate limit state of RC sections subject to axial force and biaxial bending", *International Journal for Numerical Methods in Engineering*, **72**, pp. 924-963 (2007).
2. Cedolin, L., Cusatis, G., Ecchelli, S. and Roveda, M. "Capacity of rectangular cross-sections under biaxially eccentric loads", *ACI Structural Journal*, **105**, pp. 215-224 (2008).
3. Chang, S. "Experimental studies of reinforced concrete bridge columns under axial load plus biaxial bending", *Journal of Structural Engineering*, **136**(1), pp. 12-25 (2010).
4. Fafitis, A. "Interaction surfaces of reinforced-concrete sections in biaxial bending", *Journal of Structural Engineering, ASCE*, **127**, pp. 840-846 (2001).
5. Lejano, B.A. "Investigation of biaxial bending of reinforced concrete columns through fiber method modelling", *Journal of Research in Science, Computing, and Engineering*, **4**(3), pp. 61-73 (2007).
6. Pallares, L., Miguel, P.F. and Prada, M.A.F. "A numerical method to design reinforced concrete sections subjected to axial forces and biaxial bending based on ultimate strain limits", *Engineering Structures*, **31**, pp. 3065-3071 (2009).
7. Rodriguez, J.A. and Ochoa, J.D.A. "Biaxial interaction diagrams for short RC columns of any cross section", *Journal of Structural Engineering*, **125**(6), pp. 672-683 (1999).
8. Rossi, P.P. "Evaluation of the ultimate strength of R.C. rectangular columns subjected to axial force, bending moment and shear force", *Journal of Engineering Structures*, **57**, pp. 339-355 (2013).
9. Massone, L.M., Gotschlich, N.J., Kang, T.H.K. and Hong, S.G. "Shear-flexural interaction for prestressed self-consolidating concrete beams", *Journal of Engineering Structures*, **56**, pp. 1264-1473 (2013).
10. Kwak, H.G. and Kim, J.K. "Implementation of bond-slip effect in analyses of RC frames under cyclic loads using layered section method", *Journal of Engineering Structures*, **28**, pp. 1715-1727 (2006).
11. American Concrete Institute, ACI 318-11 "Building code requirements for structural concrete and commentary", ACI 318R-11, Farmington Hill, MI, USA (2011).
12. Spacone, E., Filippou, F.C. and Taucer, F.F. "Fibre beam-column model for nonlinear analysis of R/C frames: Part I. Formulation", *Journal of Earthquake Engineering and Structural Dynamics*, **25**, pp. 711-725 (1996).
13. Limkatanyu, S. and Spacone, E. "Reinforced concrete frame element with bond interfaces. Part I: Displacement-based, force-based, and mixed formulations", *Journal of Structural Engineering, ASCE*, **128**(3), pp. 346-355 (2002).
14. Hashemi, S.SH., Tasnimi, A.A. and Soltani, M. "Nonlinear cyclic analysis of reinforced concrete frames, utilizing new joint element", *Journal of Scientia Iranica, Transactions A*, **16**(6), pp. 4901-501 (2009).
15. Hashemi, S.SH., Tasnimi, A.A. and Soltani, M. "Nonlinear analysis of three dimensional reinforced concrete frames, considering bar-concrete interaction", *Journal of Faculty of Engineering (JFE)*, ISSN: 0803-1026, **45**(2), pp. 141-154 (2011) (In Persian).
16. MathWorks, MATLAB, "The language of technical computing", Version 7.11.0. (R2010a) (2010).
17. Park, R., Kent, D.C. and Sampton, R.A. "Reinforced concrete members with cyclic loading", *Journal of the Structural Division, ASCE*, **98**(7), pp. 1341-1360 (1972).
18. Scott, B.D., Park, R. and Priestley, M.J.N. "Stress-strain behaviour of concrete confined by overlapping hoops at low and high strain rates", *ACI Journal*, **79**(1), pp. 13-27 (1982).
19. Yassin, M.H.M. "Nonlinear analysis of pre-stressed concrete structures under monotonic and cyclic loads", PhD Thesis, University of California, Berkeley, California (1994).
20. Giuffre, A. and Pinto, P.E. "The behavior of reinforced concrete to cyclic stress of strong intensity", *Journal of Genio Civile*, **5**, pp. 391-408 (1970) (in Italian).

    "Il comportamento del cemento armato per sollecitazzioni cicliche di forte intensita", Giornale del Genio Civile, Maggio (1970) (in Italian).

21. Menegoto, M. and Pinto, P. "Method of analysis for cyclically loaded RC plane frames including changes in geometry and non-elastic behaviour of elements under combined normal force and bending", *Symp. Resistance and Ultimate Deformability of Structures Acted on by Well Defined Repeated Loads*, IABSE Reports, **13**, Lisbon (1973).

22. Eligehausen, R., Popov, E. and Bertero, V. "Local bond stress-slip relationship of deformed bars under generalized excitations", Report UCB/EERC-83/23, Earthquake Engineering Center, University of California, Berkeley (1983).

23. Qiu, F., Li, W. Pan, P. and Qian, J. "Experimental tests on reinforced concrete columns under biaxial quasi-static loading", *Journal of Engineering Structures*, **24**, pp. 419-428 (2002).

24. Comite Euro International du Beton, "CEB-FIP model code for concrete structures", Paris (1978).

25. Hashemi, S.SH. and Vaghefi, M. "Investigation of the effect of a bar's inadequate embedded length on the P-M interaction curve of reinforced concrete columns with rectangular sections", *Turkish Journal of Engineering and Environmental Sciences*, **36**, pp. 109-119 (2012).

Biographies

Seyed Shaker Hashemi was born in Kazeroun, Iran, in 1981. He earned a BS degree in Civil Engineering from the Power and Water University of Technology (PWUT) in 2003, and MS and PhD degrees in Earthquake and Structural Engineering from Tarbiat Modares University, Tehran, Iran, in 2005 and 2009, respectively. He is currently Assistant Professor in the Department of Civil Engineering at the Persian Gulf University, Bushehr, Iran, and his research interests are in the areas of structural and earthquake engineering, especially nonlinear numerical analysis of reinforced concrete and the design of structures.

Mohammad Vaghefi was born in Shiraz, Iran, in 1973. He earned BS and MS degrees in Civil Engineering from Shiraz University, Iran, in 1997 and 1999, respectively, and a PhD degree, in 2009, from Tarbiat Modares University, Tehran, Iran. He is currently Assistant Professor of Civil Engineering. He has published about 58 journal papers and presented about 195 papers at national and international conferences.